

5.4 THE METEOR RADAR AS A TOOL FOR UPPER ATMOSPHERE RESEARCH

S. K. Avery

Department of Electrical and Computer Engineering
Cooperative Institute for Research in Environmental Sciences
University of Colorado, Boulder, Colorado 80309-0425

Meteor radar provide measurements of the upper mesosphere-lower thermosphere neutral wind field by using the reflection of electromagnetic waves from meteor trails. These radars are relatively inexpensive and provide an excellent means of monitoring the mean winds and tides in the 80 - 100 km region. Recently new techniques have been developed to detect meteor echoes from other ground-based radar systems operating in the HF/VHF frequency range. The meteor echo information augments the data that are routinely collected by these radars. These new techniques will be discussed.

Brief History

- 1920s - Anomalous echoes from ionosphere
- World War II - Meteors identified as source of ionization
- 1950s - Atmospheric processes studies using meteor echoes
 - Established technique

Traditional meteor radar systems

- Roper (1984)
- CW or pulsed
- Low-powered Tx
- Wide antenna beams
- Coherent receivers - Doppler detection
 - Strong signal but short-lived
- Used for mesosphere dynamics studies

Meteor detection on ST/MST and IDI radars

- Present 24 hours day⁻¹
- Augments data routinely obtained by radar

Detection on IDI radar

- Adams et al. [1986] 2.66 MHz
- Frequency-domain interferometry
- Meteor echoes extracted using power threshold algorithm
 - Time-domain interferometry for location of echo

Detection ST/MST radars

- Avery [1987]; Fukao [1987]
 - Post-processing
- Real-time detection and collection

Problems

- Narrow antenna beams
- Coherent averaging/FFT
- Strong turbulence

MEDAC (Meteor echo detection collection)

- Operates in parallel with existing radars
 - Power threshold versus partial DFT
 - Inexpensive
- Field tested on ST radar at Platteville, CO
- Performance tested on Poker Flat MST radar
- Used in support of observation campaigns

Summary

- Meteor radars are a good measurement technique for studying mean winds, tides, planetary scale waves, long period gravity waves.
- ST/MST and IDI radars receive meteor echoes.
- With optimum detection, collection, and signal processing of these echoes, additional data can be obtained that augments the normal data taken by these radars.

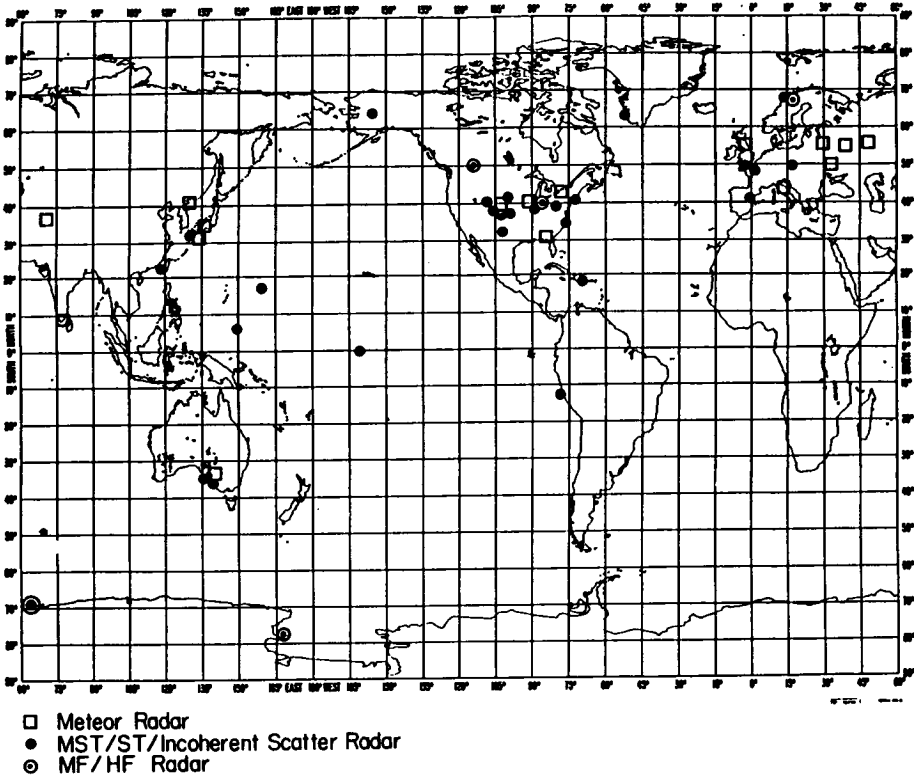


Figure 1. Geographic distribution of currently operating meteor radars, MST/ST/incoherent scatter radars, and MF/HF radars. Meteor radars are an established technique for studying the upper mesosphere/lower thermosphere.

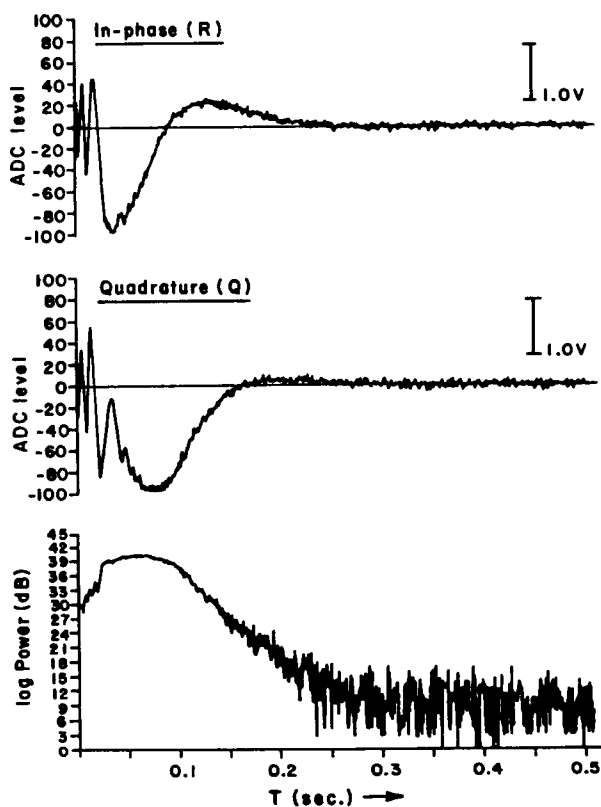


Figure 2. Output from the coherent receiver and power due from a meteor echo. The transmitted radar signal is scattered from free electrons associated with the ionized meteor trail. The fast rise time in the power is a function of the meteor velocity. The exponential decay in power is due to the diffusion of the trail. The high frequency in the voltage is due to the formation process of the first Fresnel zone of the diffraction pattern of the echo. The low frequency observed after the power has reached the peak is due to the neutral wind.

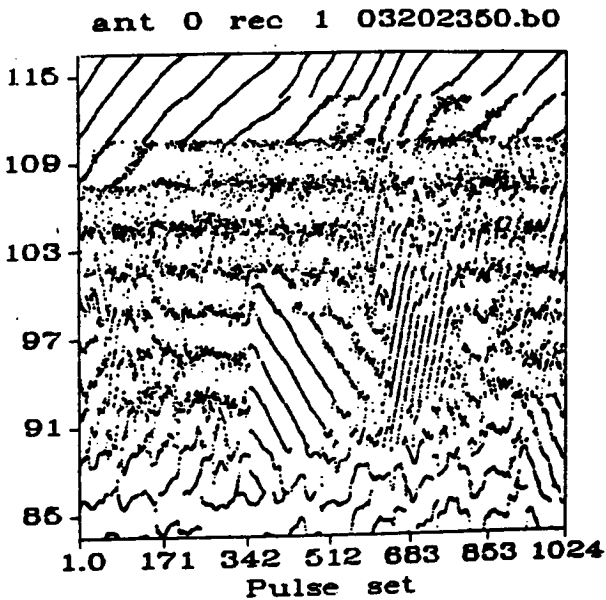
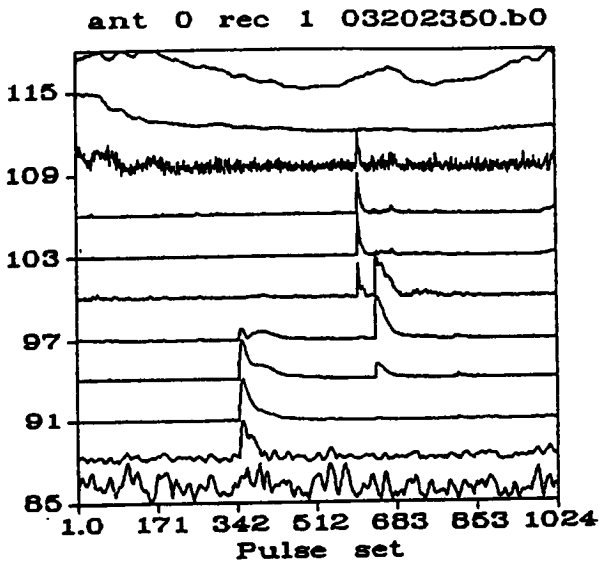


Figure 3. From Turek [1986]. Amplitude and phase of echo received on IDI radar. Meteor echoes are seen easily in the amplitude plot. For these echoes a clear phase progression is observed.

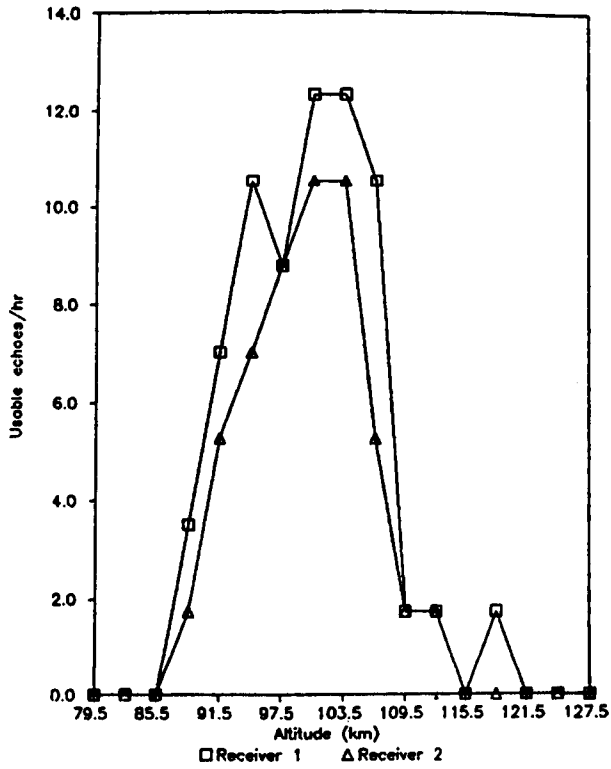


Figure 4. Meteor echo rate as a function of height for echoes observed on 2.66 MHz IDI radar [Turek, 1986]. Peak echo rate occurs at 103 km.

ORIGINAL PAGE IS
OF POOR QUALITY

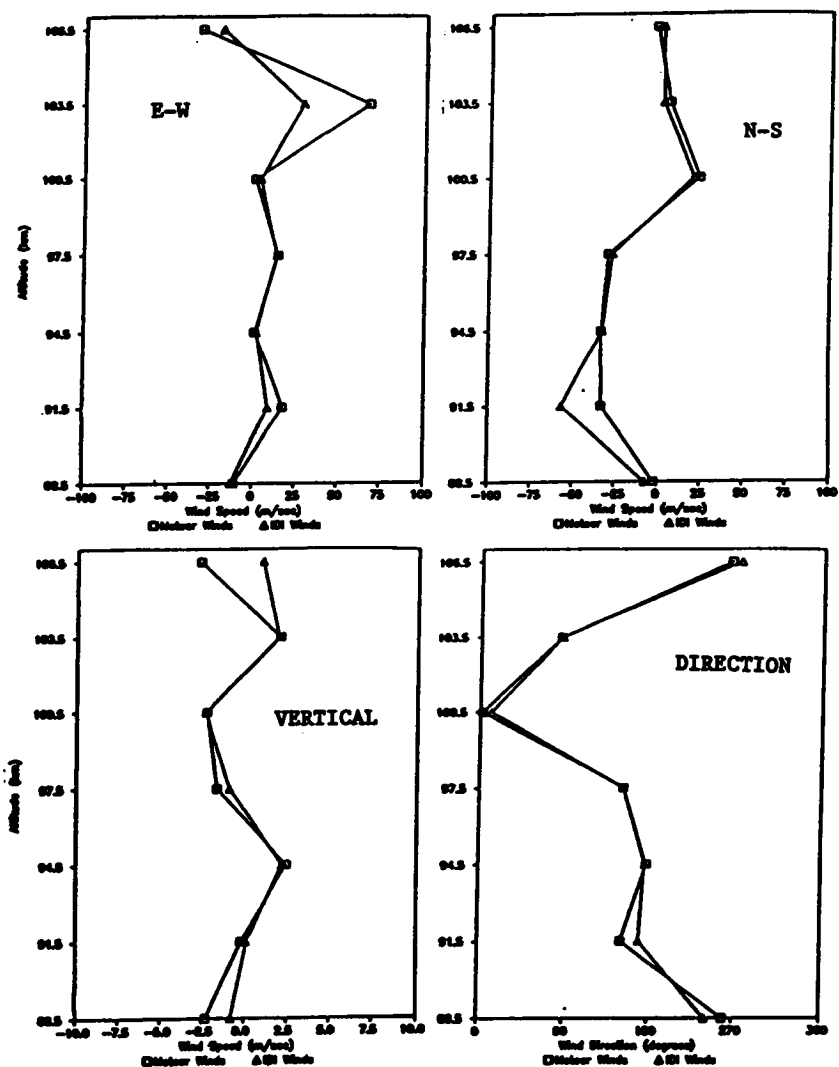


Figure 5. Comparison of winds derived from meteor echoes and those derived from regularly collected echoes on IDI radar.

ORIGINAL PAGE IS
OF POOR QUALITY

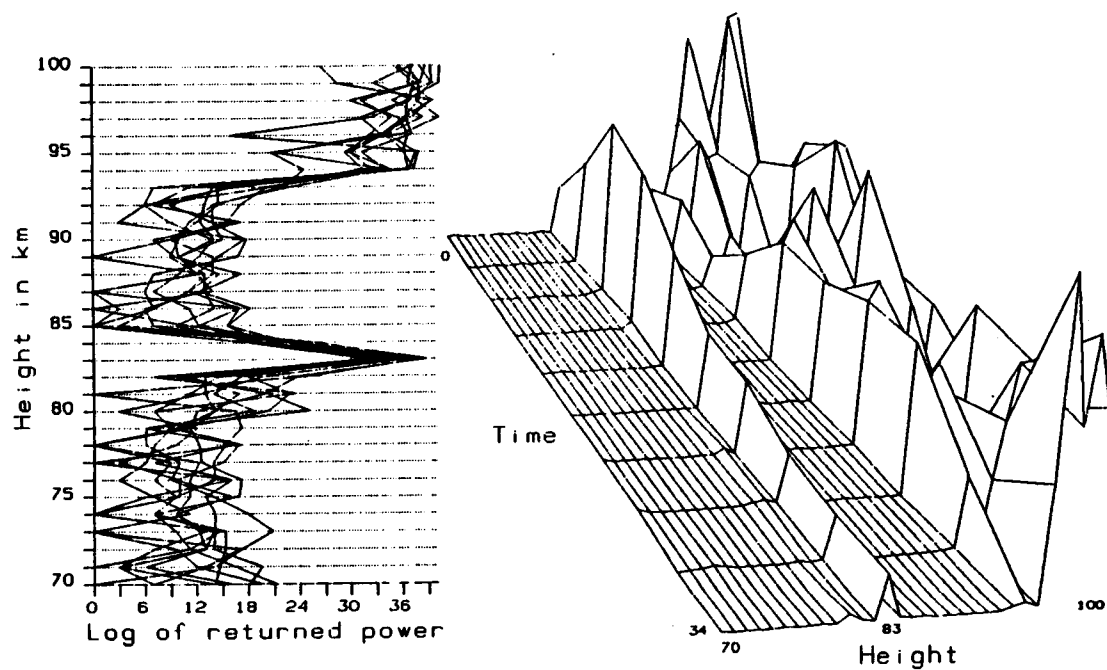


Figure 6. Profile of meteor echo observed at Jicamarca Radio Observatory. Power at the upper altitudes is due to the electrojet.

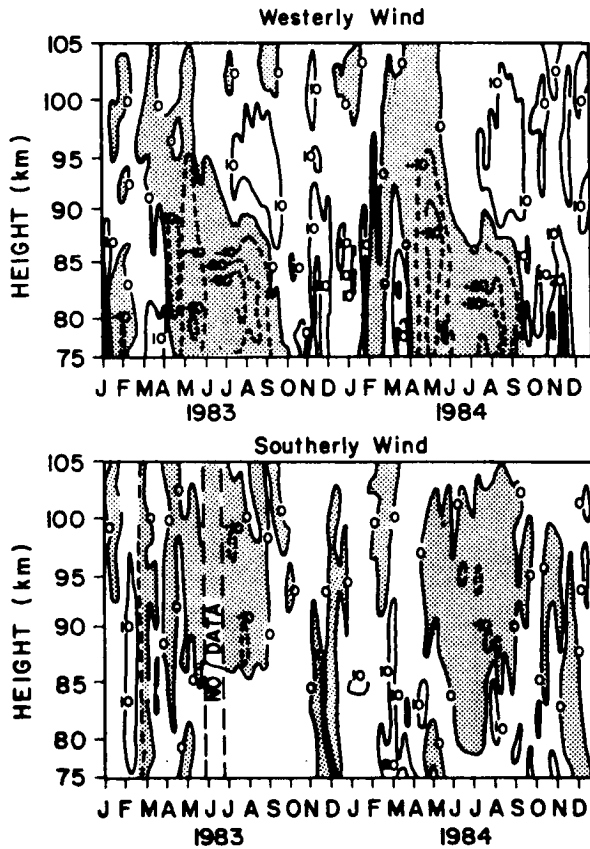


Figure 7. From Manson, et al. [1988]. Mean winds determined from meteor echoes observed on the Poker Flat, Alaska MST radar.

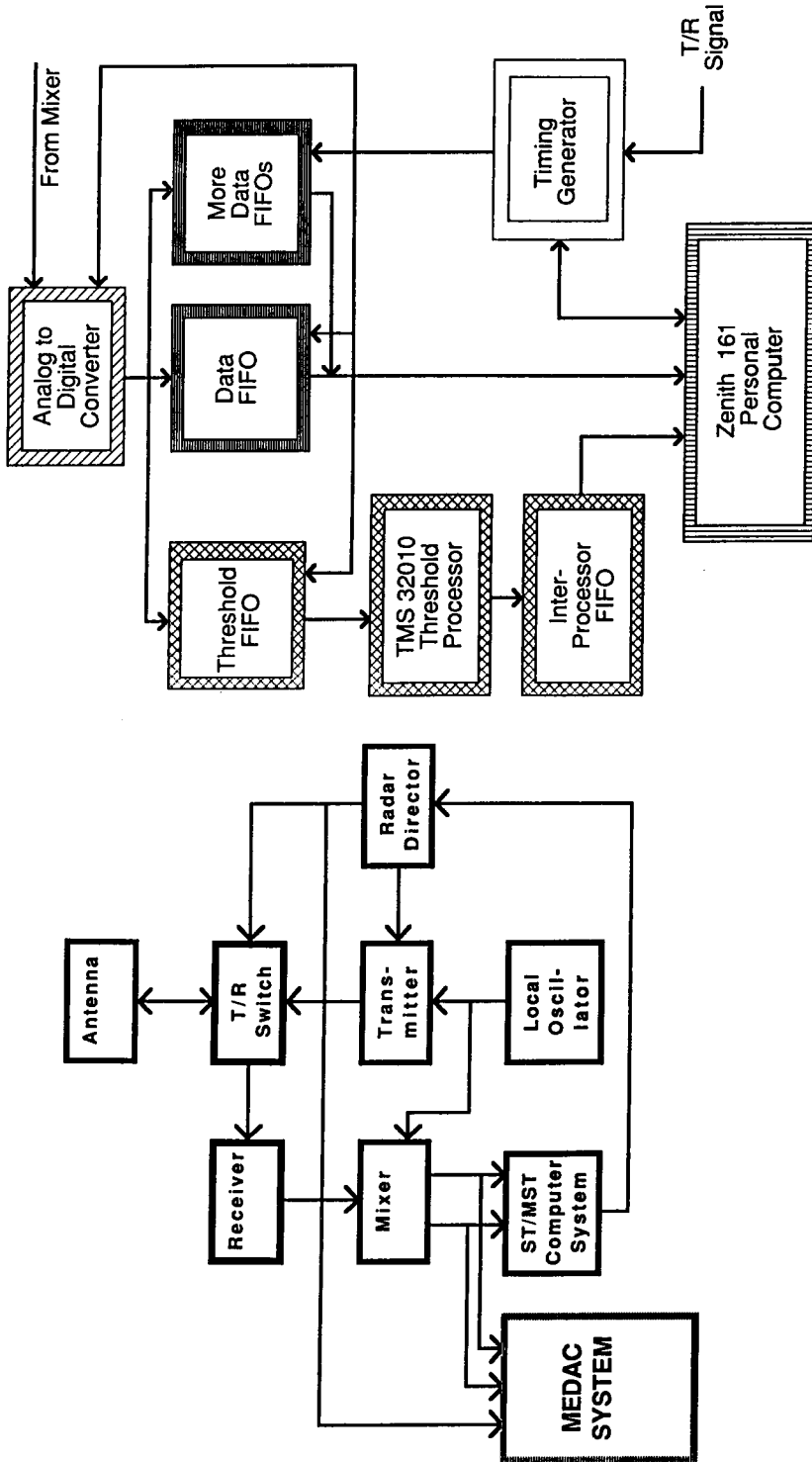


Figure 8. Block diagram of MEDAC connections to the radar.

Figure 9. Block diagram of MEDAC system.

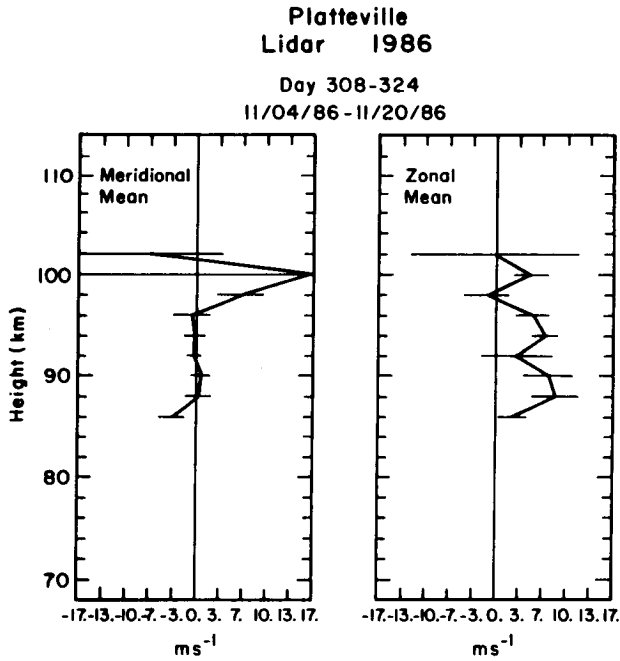


Figure 10. Mean winds from MEDAC system operating on Platteville, CO, ST radar. This observational campaign was carried out in coordination with the sodium lidar from the University of Illinois.

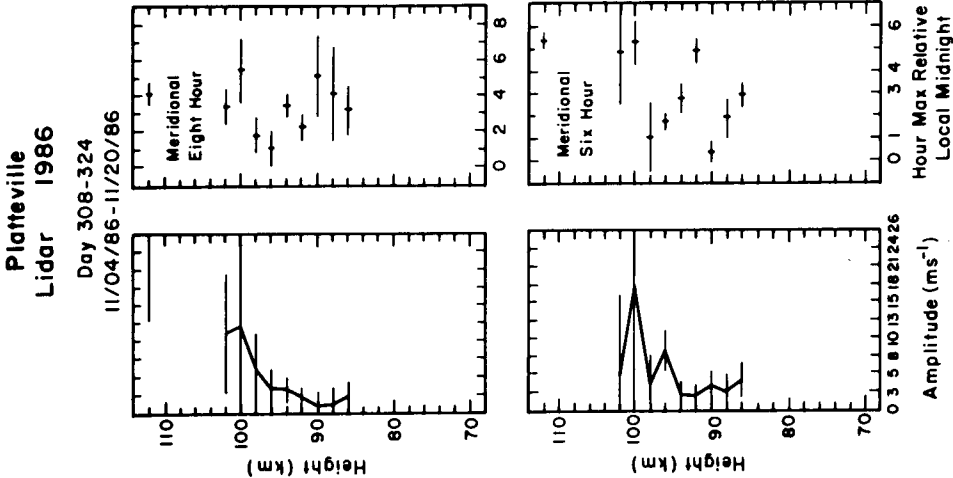


Figure 12. Eight- and six-hour components of wind field. The six-hour component was also observed with the sodium lidar.

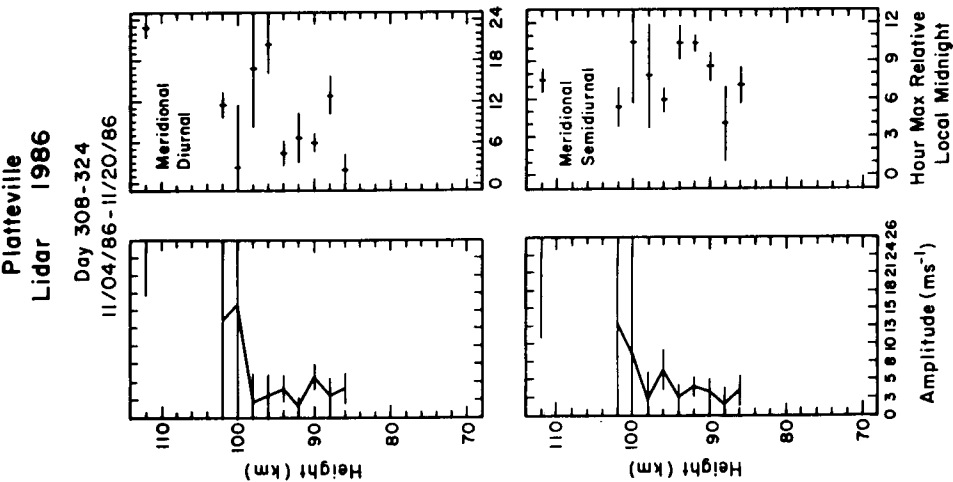


Figure 11. Amplitude and phase of the diurnal and semidiurnal tide during the same period as in Figure 10.

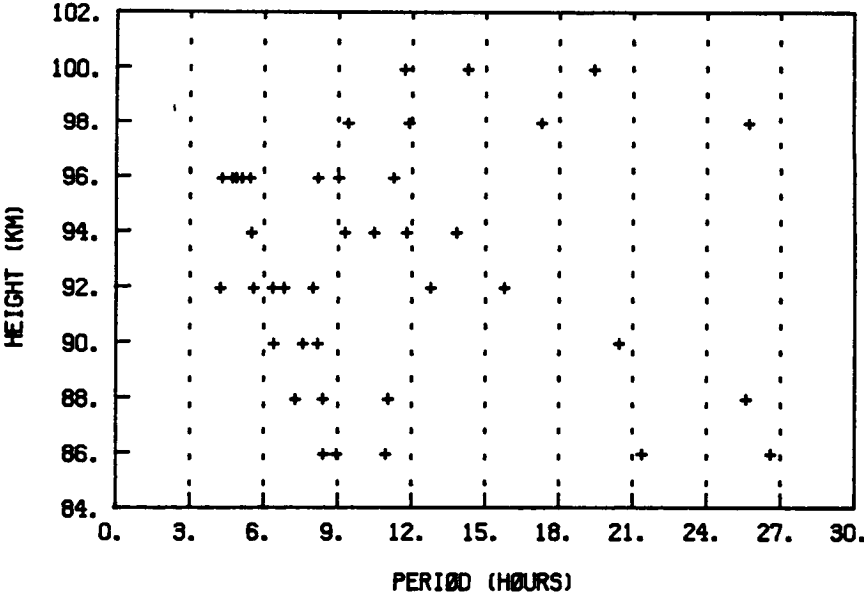


Figure 13. Period estimates of wave motions determined using a new algorithm for randomly sampled data, signal processing improvements can enhance the use of meteor radar data.